

# ANALYSIS OF FLUID-STRUCTURE INTERACTION IN MICROMIXERS WITH VIBRATING WALLS

Madhumitha Ravichandran<sup>1</sup>, Arunkumar Seshadi<sup>2</sup>, Ravichandran V<sup>3</sup> and Venkatesan Muniyandi<sup>1,\*</sup>

\*Author for correspondence

<sup>1</sup>School of Mechanical Engineering, SASTRA University, Thanjavur, Tamilnadu, India

<sup>2</sup>Dept of Applied Mechanics, Indian Institute of Technology Madras, Chennai, India

<sup>3</sup>PG Senapathy Centre for Computing, Indian Institute of Technology Madras, Chennai, India

E-mail: [mvenkat@mech.sastra.edu](mailto:mvenkat@mech.sastra.edu)

## ABSTRACT

Rapid mixing in micro-channels plays a significant role in the chemical, biological and medical fields. The majority of microfluidic applications is encountered in very low Reynolds number regime. Thus, two reactive fluids are predominantly parallel when they flow along the length of the microchannel. Generally, obstacles or surface modifications are made in the flow path to increase mixing of the fluids. With the development of deformable and flexible micro-channels, the focus has now shifted to the development of micromixers with moving or vibrating walls. In the present work an attempt has been made to numerically model the working of a micromixer with vibrating walls. This has been accomplished by computationally solving the coupled set of equations governing the elasticity of the walls and fluid motion (Fluid structure Interaction). Mixing index, which is a measure of effectiveness of mixing is calculated based on the species concentration at a particular region of interest. External sinusoidal vibrations are applied on the walls of the microchannel of size 225  $\mu\text{m}$ . The effect of vibration on mixing index is studied. Optimization study is taken up to obtain the optimal value of vibration amplitude and frequency to achieve enhanced mixing with reduced pressure drop. The optimal parameters so obtained are observed to function well in the Reynolds number range 0.5-50 in which the entire numerical analysis has been carried out

## INTRODUCTION

Microreaction technology [1] has enormous applications in the field of chemical and biological sciences. Increased surface to volume ratio in microchannel leads to high heat and mass transfer rates, which makes it more suitable for chemical reactions than conventional channels. A few applications in which microreaction technology has proved its impact include biological screening, polymerization, protein folding, drug delivery and organic compound synthesis. Several advantages of the micro total analysis system ( $\mu$ -TAS) include an abated amount of sample and reagent volume consumption, low cost, reasonable portability and augmented reaction time [2]. However, the flow behaviour in microchannels limits the development in the field of microfabrication technology. The flow through a microchannel occurs at very low Reynolds numbers. Most flows in microchannels are observed in low laminar or creeping regimes. Thus the flow of two fluids during reaction is predominantly parallel or separated [3]. The separated

flow of the two components reduces the pervasion of one flow stream component into the other which slows down the chemical reaction rate. This necessitates development of a device which induces chaos or diffusion in the fluid regime that enhances mixing. Micromixer [4] is an important component in chemical reaction technology that performs the task of inducing chaos or diffusion to achieve rapid mixing between the fluids. Effective mixing is established in micromixers of two kinds, active and passive [5]. Active micromixers use external force which may be electric [6], magnetic [7] or acoustic in nature [8] to induce chaos in the flow regime. In passive mixers, mixing occurs by virtue of modification in geometry and spatial orientation that either induces re-circulations or increases the effect of diffusion [9].

The primary objective of a passive micromixer is to increase the contact surface between the fluids by modifying the flow surfaces. The most primitive design of a passive micromixer essentially implements parallel laminations [10]. In this type of micromixer, a single inlet fluid stream is divided into multiple streams which are combined together later. This induces increased diffusion at the downstream of the flow channel. Different modifications were made to parallel micromixers and were presented in detail in [11-12]. In one such modification called injection micromixers, solute flow alone is divided into sub-streams which are later injected into the solvent [13]. The injection of solutes into solvent is carried out using nozzles. The above concepts were based on diffusion of one component into another. Yet another way of classifying micromixers could be based on the nature and magnitude of chaos induced in the flow field. A few examples of these micromixers include mixers with cylindrical obstacles [14], zig-zag micromixers [15] and micromixers with tesla structures. The latter class of micromixers that induce chaotic advection are quite desirable in very low flow rate applications where enhancement of diffusion is difficult. However, these micromixers face a major drawback because they have a large pressure drop associated with them.

In the present work, an attempt is made to strengthen the concept of vibrating micromixers. Developments in material science in micro-environment have led to the use of deformable or flexible micromixers [16-17]. In the present work, an attempt is made to numerically model the working of a micromixer with vibrating walls and to optimize the physical variables such as vibration frequency and amplitude. Finite element modelling of fluid structure interaction is done to study the enhancement of mixing in micromixers with vibrating walls. Working physics of the vibrating wall micromixers is elucidated and the parametric

dependence of the associated physical variables on the mixing effectiveness is described.

## NUMERICAL MODEL

In the present work, a microchannel with a T shaped mixer section is used to allow the two fluids to enter inside the flow channel. The mixing channel has a cross-section width of 225  $\mu\text{m}$ . The walls of the microchannel at downstream to the T-junction are deformable. The material properties of the deformable wall are taken from literature and are shown in table 1. The entire T shaped microchannel is kept inside a fluidic domain. In the present work, the walls of the microchannels vibrate as a result of sinusoidal impact provided by the fluid motion. In the present case water flows at high velocity and frequency which provides impact on the walls to causes vibrations. Moreover, in reality the mechanism to provide actuation could be fluidic as in the present case or acoustics, electrical or magnetic in nature. The nature of the actuating force has to be chosen based on the material properties of the deformable wall. The entire numerical setup comprising of the vibrating walls and the flow through the micromixer is modelled as shown in Figure 1. The exterior walls of the fluid domain are prescribed a mesh displacement of zero. There are four fluid inlets. The two inlets (a&b) at the ends of T shaped microchannel provide entry to the reactive fluids into the mixer sections. The other two inlets (c&d) are provided for the sinusoidal fluid actuation.

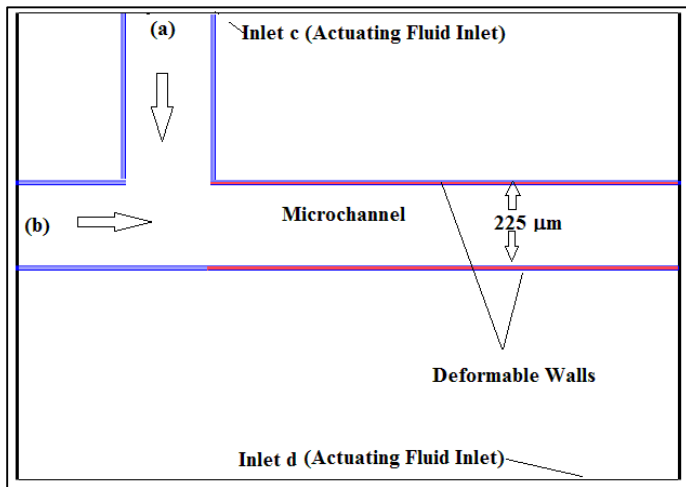


Figure 1. Numerical Model

The entire numerical model was created and tested using the commercial finite element based solver COMSOL MULTIPHYSICS ©. A triangular mesh comprising of 1112035 elements is used after performing a grid independence test. The Reynolds number of the flow through the microchannel is taken to be in the range 0.05-50. Mass and momentum conservation equations shown in Eqn.1 and Eqn. 2 are coupled and solved with the species transport equation shown in Eqn.3 in the flow field. Two fluids are modelled with different concentrations of dilute species based on the inlet mass fraction of dilute species

in both the fluids. The concentration of the fluid at a particular location is modelled using transport of dilute species equation shown in Eqn 3. The Continuity equation is given as:

$$\rho \cdot \nabla \cdot u_{fluid} = 0 \quad (1)$$

The Navier-Stokes equation is given as:

$$\rho \frac{\partial u_{fluid}}{\partial t} + \rho(u_{fluid} \cdot \nabla)u_{fluid} = \nabla \cdot [-p + \mu(\nabla u_{fluid} + (\nabla u_{fluid})^T)] \quad (2)$$

Species transport equation is given as

$$\frac{\partial C}{\partial t} = \nabla \cdot (D \nabla C - uC) \quad (3)$$

Table 1. Material Properties of Vibrating walls

Property Name	Value
Young's Modulus	$2 \times 10^5$ Pa
Poisson ratio	0.33
Density	$7850 \text{ kg/m}^3$
Wall thickness	$10 \mu\text{m}$

Here D is the diffusivity of the medium, C is the concentration and  $u = u_{fluid}$ . The value of D can be inferred from Eqn. 4 where  $k_b$  is Boltzmann constant,  $T_0$  is the ambient temperature (25°C) and  $d_h$  is the hydrodynamic diameter of the particle (200 nm). The concentration at one inlet is considered as  $1 \times 10^6 \text{ mol/m}^3$  and other as 0. The value of inlet concentration is calculated based on the mass fraction of dilute species. Concentration 0 in the second inlet indicates that the mass fraction of the dilute species in the second inlet is zero. Concentration value for other inlet is obtained for 0.02 % of dilute species.

$$D = \frac{k_b T_0}{3\pi\eta d_h} \quad (4)$$

As the fluidic channel is kept inside a fluidic domain, the walls of the channel which are solid have an interface with the fluidic domain. At this solid-fluid domain, a coupled interaction is modelled and solved in a sequential order of steps. Hence the equation at the deformable walls is calculated from coupled fluid-structure interaction equation. They are shown below.

$$u_{fluid} = u_w \quad (5)$$

$$u_w = \frac{\partial u_{solid}}{\partial t} \quad (6)$$

$$\sigma \cdot n = \Gamma \cdot n \quad (7)$$

$$\Gamma = [-p + \mu(\nabla u_{fluid} + (\nabla u_{fluid})^T)] \quad (8)$$

Here  $\sigma$  is the surface tension. The velocity of wall  $u_w$  is 0 initially before the impact of the oscillating fluid which causes the impact.

As suggested earlier, the walls are made of compliant and deformable material. In order to study the dynamics of the channel walls, linear elastic model and the governing equations are shown below

Mixing index is used to calculate the local efficiency of mixing at the post mixing zone. Mixing index of 0 indicates complete mixing. It has to be understood that the mixing index is calculated at the outlet.

$$\begin{aligned} \rho \frac{\partial^2 u_{solid}}{\partial t^2} &= \nabla \cdot \sigma = F_v; \quad \sigma = (s \cdot (\nabla u_{solid})) \\ S - S_0 &= \varepsilon - \alpha (T - T_{ref}) - \epsilon_0 \\ \epsilon &= \frac{1}{2} (\nabla u_{solid})^T + \nabla u_{solid} + (\nabla u_{solid})^T \nabla u_{solid} \end{aligned} \quad (9)$$

$$M = \frac{\sum \text{Elements in Section 3} \frac{|C - C_{avg}|}{C_{avg}}}{\text{Number of Elements in Section 3}} \quad (10)$$

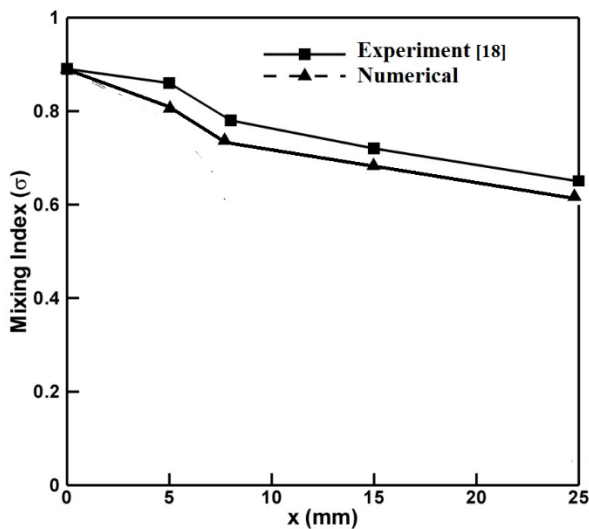


Figure 2. Validation

Here  $C_{avg}$  is the concentration of the fluidic medium at a local space when the fluids are completely mixed. In the present case it is the arithmetic mean of both the inlet configurations. PARDISO solver is used to solve the discretised finite element equations. The fluid structure interaction problem at the fluid – solid interface (deformable walls) is modelled in three consecutive steps. Solution is run till convergence is achieved. The numerical model is validated with a small lab scale microchannel fabricated using PDMS as presented by Asfer and Panigrahi [18]. The graph for validation in terms of variation in mixing index with distance of the medium is shown in figure 2. As the fluid structure problem involves changing the shape of the walls at every time interval, the mesh is updated with implicit mesh movement in accordance with the velocity of the walls. The frequency of vibration and amplitude are changed by

varying the mean velocity and frequency of the sinusoidal velocity input.

## RESULTS AND DISCUSSION

### FLOW THROUGH CHANNEL WITH NON DEFORMABLE WALL

Initially analysis is done to study the extent of diffusion in microchannels with non-deformable wall. As the two fluid flow components which are of comparable densities flow through the T-section, it is seen that flow separates in the two streams from each other. There is some intermittent mixing at the interface because of diffusion between the two components. As the two components flow through the channel, the amount of mixing increases as shown in Figure 3. This can be attributed to the increase in diffusion with the length of the flow channel. Due to the micrometer scale of the system geometry taken at low flow rates, it was seen that the value of Peclet number is much higher than unity (100-1000). Peclet number gives the ratio of mass transfer contribution by convection to that by diffusion. This indicates that the contribution of convective transfer to mass transfer is higher when compared to the magnitude of mass transfer by diffusion. This causes separation of the two streams in the flow channel. The typical diffusion length scale is given by Eqn. 11.

$$L_{diff} = 2\sqrt{DT} = 2\sqrt{\frac{L}{U}} \quad (11)$$

The extent of diffusion in mixing is said to be high when the diffusion length is greater than the diameter of the channel. When there is an increase in length of the channel or decrease in velocity, there is an increase in diffusion length. However, inlet velocity is a physical state variable in chemical reactions and is chosen based on a requirement for a particular set of reactions. Figure 3 also shows the effect of increase in Reynolds number on micromixing. It was seen that with the increase in Reynolds number, there is initially a decrease in mixing. This results due to the decrease in diffusion length because of mixing. However, with further increase in Reynolds number ( $Re > 10$ ), there is an increase in amount of mixing.

This interesting phenomenon can be explained based on formation of local vortices and instabilities in the T shaped mixer section. Thus, there is a transition from unmixed parallel flow to mixed flow when the Reynolds number is sufficiently high. Though it can be seen that, there is an enhanced mixing in microchannels at high Reynolds number, the operability of microchannels at high flow rates is less. This is because of the phenomenally high pressure drop arising in the microchannels to pump fluids at such high flow rates.

### FLOW THROUGH CHANNEL WITH PERMANENTLY DEFORMED WALL

It can be seen from Equation 11 and the description in the previous section, that there are two factors to be considered to

increase the extent of mixing; one is to increase the ratio of length of diffusion to size of the flow channel and the other is to increase the Reynolds number to the extent of producing chaos. In the present work, both these factors are taken into consideration. The walls of the microchannel are made to deform at the center of the channel. As the wall deforms, the size of the flow channel at the local deformation space is reduced as shown in Figure 4. Thus the ratio of Length of diffusion to size of the channel is increased. This causes an enhanced mixing in the flow channel. The variation in mixing index with distance is shown in Figure 5. Figure 5 also shows the variation in mixing index with change in deformation height ( $\epsilon$ ). It can be seen that with increase in deformation height till a certain extent, there is an enhancement in the mixing index. This is because of the increase in the ratio of diffusion height to the size/diameter of the microchannel. Here axis length corresponds to length along X axis.

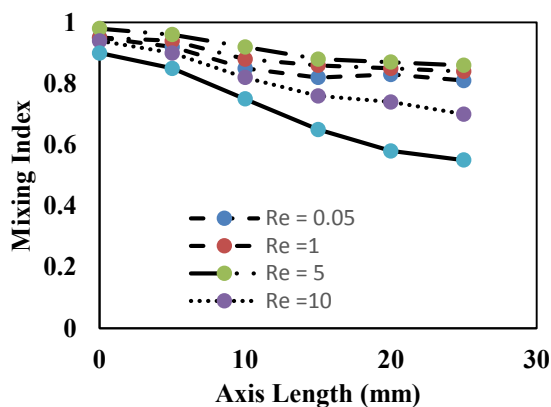


Figure 3. Mixing index in flow through Non-deformable channel

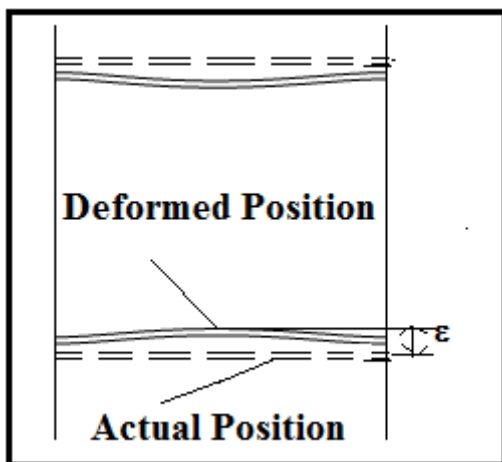


Figure 4. Section View of the deformed wall

However, when the deformation height increases more than the level as shown in Figure 5, there is a steep increase in local Reynolds number due to flow constriction. This causes an increase in convective transport of mass. Thus the value of Peclet number increases. Hence the amount of mixing considerably decreases. The variation in Peclet number with deformation height is shown in Figure 6. It can be seen from Figure 5 and

Figure 6, that there is an optimal height of deformation that provides the maximum mixing.

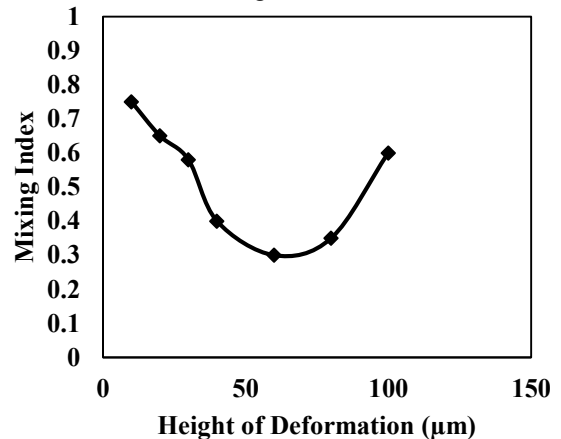


Figure 5. Variation in Mixing Index with Height of Deformation with permanent deforming walls

Thus, it can be concluded that the optimal value of height of deformation can be obtained by studying the contrasting effects of increase in diffusion length to size of the channel and increase in Peclet number. It can be seen that with the introduction of deformation in the walls of the microchannels, there is a pronounced effect on the mixing of the microchannels. An optimal value of deformation height produces enhanced mixing in the microchannels. However, there is an inherent disadvantage associated with the permanent deformation in the wall. There is a steep increase in the pressure drop inside the flow channel. The steep increase in pressure drop in the microchannel is highly undesirable as described earlier. Therefore, in the present case, an attempt is made to have a wall that deforms periodically. In other words a micromixer with vibrating channel walls is considered as an alternative to the micromixer with deformed walls.

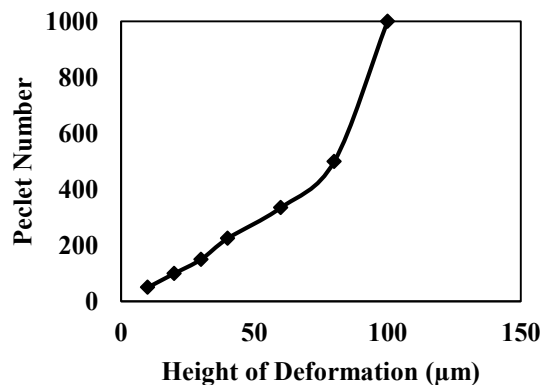


Figure 6. Variation in Peclet number with Height of Deformation

## FLOW THROUGH CHANNEL WITH VIBRATING WALLS

In the present case, a half sinusoidal velocity is provided on to the actuating fluid (Water in the present case) that causes the wall vibration. A half sinusoidal inlet velocity condition is

provided to avoid the need to have a bidirectional movement of velocity at the inlet which is difficult to be attained in real time. Thus the velocity at the inlet varies from 0 to  $U_{max}$  where  $U_{max}$  is the velocity amplitude of the actuating fluid. When the instantaneous velocity of the actuating fluid at the fluid inlet is  $U_{max}$ , the deformation of the wall is maximum and when the velocity decreases to zero, the fluid flowing through the microchannel causes the walls to return to the original position. This process is repeated at the specified frequency. The wall deformation at various conditions are shown in Figure 7.

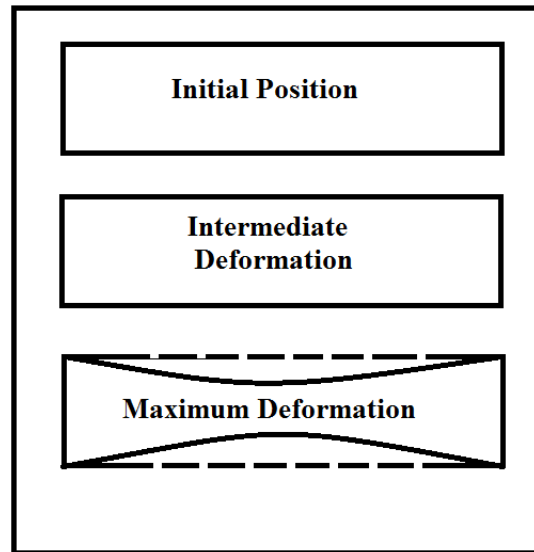


Figure 7 Various Positions of wall during Vibration

The variation in mixing index along the length of the channel for micromixer with vibrating walls is shown in Figure 8. It can be seen from Figure 8 that as the flow passes through the deformation zone there is an increase in amount of mixing. This can be explained based on the increase in ratio of diffusion length to size of the microchannel. The two guiding parameters involved in the functioning of micromixer with vibrating walls are amplitude and frequency of wall vibration. In the present case, the frequency of wall vibration is the same as that of the frequency of actuating fluid inlet. The amplitude of vibration can be linked with maximum deformation of the microchannel. However, the amplitude and frequency of vibrations are constrained by the material nature of the microchannel walls. Vibration frequency cannot exceed the resonant frequency of the wall material. Similarly, the deformation height is constrained based on the elastic strength of the micromixer walls. In the present case, the frequency of vibration is in the range 10-100 Hz and the deformation height is 10-100  $\mu\text{m}$ . It should be remembered that the size of the microchannel is 225  $\mu\text{m}$ . This range is assumed based on the restriction specified above.

#### PARAMETERIC DEPENDENCE AND OPTIMIZATION

Figure 9 shows the effect of wall deformation height on the mixing index. It is seen from Figure 9, that the average mixing index is at the maximum when the wall deformation is around 76

$\mu\text{m}$  which is roughly 0.675 times the size of the microchannel. This can be accounted for based on the analysis performed in the previous section. It has to be recollected that with further increase in height of deformation, the pecllet number increases drastically leading to convective dominance in the flow channel. This causes reduced mixing. Figure 10 shows the effect of vibration on the mixing index. It can be seen from the figure that with increase in frequency of vibration (<60 Hz) there is enhanced mixing in the flow channel. It is seen from the numerical analysis at frequencies in the range (30-60 Hz), that there is formation of local vortices at the vicinity of the deformation regions. These vortices are found to enhance the mixing effect which adds to the contribution of diffusion aided mixing.

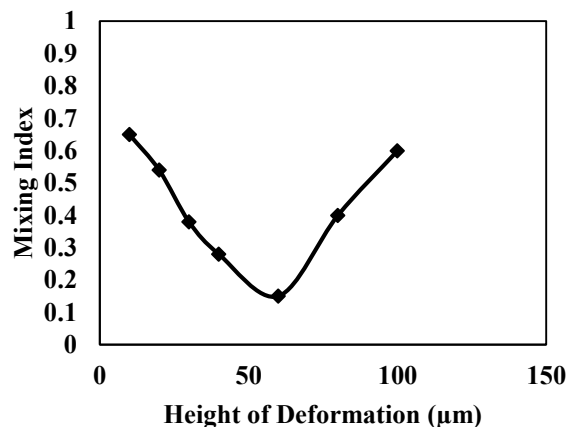


Figure 8. Effect of Height of deformation in Vibrating wall micromixer (Frequency = 60 Hz)

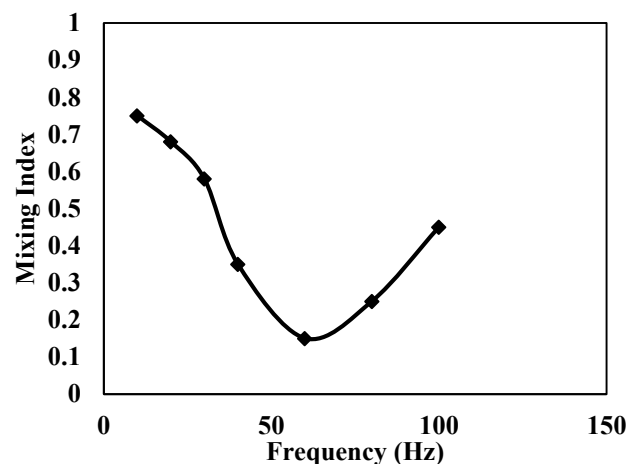


Figure 9. Effect of Frequency of deformation in Vibrating wall micromixer (Height = 75  $\mu\text{m}$ )

With increase in frequency above 60 Hz, there is a gradual decrease in mixing. This is because of the fact that the time to attain maximum deformation is less than the diffusion time required to achieve the desired diffusion length. Thus, in the case of high frequencies, the extent of diffusion decreases leading to decreased mixing. Thus it can be ascertained that in the present



work, micromixer with walls vibrating at 60 Hz provides the maximum augmentation in mixing when the deformation height is around 0.675 times the radius of the micromixer. The efficiency of these optimal parameters for various Reynolds numbers is studied. It can be seen from Figure 10, that the obtained optimal physical parameters provide an enhanced mixing in the tested Reynolds number range ( $Re = 0.05$  to 50).

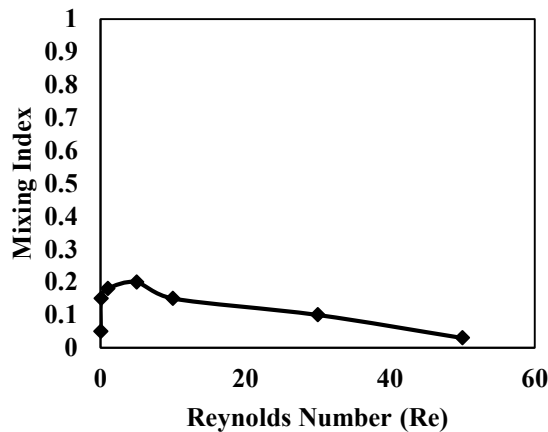


Figure 10. Operability at different Reynolds number

The present analysis is extended to tubes of different sizes ( $d$ ) in the range 100-1000  $\mu\text{m}$ . The range of optimal parameters of the associated physical variables are described in table 2. It is seen from the numerical analysis that micromixers with vibrating walls provide the maximum mixing when operated in the range specified in table 2.

Table 2. Range of Optimal Parameters

Parameters	Frequency	Deformation Height
Values	40-60	$d/4-d/3$

## CONCLUSION

In the present work, a micromixer design is presented that uses vibrating walls to enhance mixing. The working of the design is studied using Finite element based numerical simulations. It is concluded from the extensive numerical analysis that the micromixer with vibrating walls provides enhanced mixing because of the increase in the ratio of length of diffusion to size of the channel. The parametric dependence of frequency and amplitude of vibration on the mixing efficiency is studied and the range of optimal parameters is obtained based on this analysis. It has been seen that with increase in frequency up to a certain limit, there is an increased mixing. However, decreased time for diffusion leads to a decreased mixing when the frequency is further increased. Similarly it was seen that there is effective mixing when the maximum height of mixing is within a specified range which allows optimal diffusion of component between the two fluids.

## REFERENCES

- [1]Löwe, H., and W. Ehrfeld. "State-of-the-art in microreaction technology: concepts, manufacturing and applications." *Electrochimica Acta* 44.21 (1999): 3679-3689.
- [2]Reyes, Darwin R., et al. "Micro total analysis systems. 1. Introduction, theory, and technology." *Analytical chemistry* 74.12 (2002): 2623-2636.
- [3]Ansari, Mubashshir Ahmad, and Kwang-Yong Kim. "Shape optimization of a micromixer with staggered herringbone groove." *Chemical Engineering Science* 62.23 (2007): 6687-6695.
- [4]Nguyen, Nam-Trung, and Zhigang Wu. "Micromixers—a review." *Journal of Micromechanics and Microengineering* 15.2 (2004): R1.
- [5]Hessel, Volker, Holger Löwe, and Friedhelm Schönfeld. "Micromixers—a review on passive and active mixing principles." *Chemical Engineering Science* 60.8 (2005): 2479-2501.
- [6]Tai, Chang-Hsien, et al. "Micromixer utilizing electrokinetic instability-induced shedding effect." *Electrophoresis* 27.24 (2006): 4982-4990.
- [7]Affanni, Antonio, and Giovanni Chiorboli. "Development of an enhanced MHD micromixer based on axial flow modulation." *Sensors and Actuators B: Chemical* 147.2 (2010): 748-754.
- [8]Liu, Robin Hui, Ralf Lenigk, and Piotr Grodzinski. "Acoustic micromixer for enhancement of DNA biochip systems." *Journal of Micro/Nanolithography, MEMS, and MOEMS* 2.3 (2003): 178-184.
- [9]Tofteberg, Terje, et al. "A novel passive micromixer: lamination in a planar channel system." *Microfluidics and Nanofluidics* 8.2 (2010): 209-215.
- [10]Wu, Zhigang, and Nam-Trung Nguyen. "Convective-diffusive transport in parallel lamination micromixers." *Microfluidics and Nanofluidics* 1.3 (2005): 208-217.
- [11]Bourne, John R., and Shengyao Yu. "Investigation of micromixing in stirred tank reactors using parallel reactions." *Industrial & engineering chemistry research* 33.1 (1994): 41-55.
- [12]Capretto, Lorenzo, et al. "Micromixing within microfluidic devices." *Microfluidics*. Springer Berlin Heidelberg, 2011. 27-68.
- [13]Coleman, Jeffrey T., and David Sinton. "A sequential injection microfluidic mixing strategy." *Microfluidics and Nanofluidics* 1.4 (2005): 319-327.
- [14]Wang, Hengzi, et al. "Optimizing layout of obstacles for enhanced mixing in microchannels." *Smart materials and structures* 11.5 (2002): 662.
- [15]Mengeaud, Virginie, Jacques Josserand, and Hubert H. Girault. "Mixing processes in a zigzag microchannel: finite element simulations and optical study." *Analytical chemistry* 74.16 (2002): 4279-4286.
- [16]Riahi, Mohammadreza, and Elaheh Alizadeh. "Fabrication of a 3D active mixer based on deformable Fe-doped PDMS cones with magnetic actuation." *Journal of Micromechanics and Microengineering* 22.11 (2012): 115001.
- [17]Effenhauser, Carlo S., et al. "Integrated capillary electrophoresis on flexible silicone microdevices: analysis of DNA restriction fragments and detection of single DNA molecules on microchips." *Analytical Chemistry* 69.17 (1997): 3451-3457.
- [18]Asfer, M., and Panigrahi, P. K. "μ-scale LIF and PIV investigation of mixing in a ribbed micromixer", EXHFT-7, 28 June – 03 July 2009, Krakow, Poland.